Hindawi
Wireless Communications and Mobile Computing
Volume 2022, Article ID 7654456, 16 pages
https://doi.org/10.1155/2022/7654456

Research Article

MMW-NOMA: An Uplink NOMA Communication System Based on the Node Pairing Algorithm of Maximum and Minimum Weight in Underwater Acoustic Networks

Guohong Gao,[1,2] Jianping Wang,[2,3] Xuejun Chen,[4] Quan Liu,[1] Ruizhi Zhai,[5] and Jianwei Ma[3]

[1]*School of Information Engineering, Wuhan University of Technology, Hubei, Wuhan 430070, China*
[2]*School of Information Engineering, Henan Institute of Science and Technology, Xinxiang, Henan 453003, China*
[3]*School of Information Engineering, Henan University of Science and Technology, Luoyang, Henan 471000, China*
[4]*School of Information Engineering, Luohe Vocational Technology College, Luohe, Henan 462000, China*
[5]*College of Mechanics and Materials, Hohai University, Nanjing 211100, China*

Correspondence should be addressed to Jianping Wang; xunji2002@163.com

Received 17 January 2022; Revised 8 May 2022; Accepted 16 June 2022; Published 30 June 2022

Academic Editor: Omprakash Kaiwartya

In orthogonal multiple access (OMA) communication systems, resources are allocated to numerous users based on time, frequency, or code domains. The low bandwidth of the underwater acoustic network limits the number of nodes that can be supported by the OMA system, due to limited resources. The innovative concept of nonorthogonal multiple access (NOMA) provides a solution that offers more nodes and increases spectral efficiency. As a promising technique, it optimizes power allocation through channel characteristics and adopts serial interference cancellation algorithms to decode the signal at the receiver. This paper introduces an underwater communication system based on the node pairing algorithm of maximum and minimum weight (MMW-NOMA). First, we build the system model in a UAN scenario. Second, we present the node pairing strategy. Third, we design a node replacement mechanism. Furthermore, we offer a power allocation algorithm. Finally, we compare the performance of MMW-NOMA with randomly paired NOMA (RP-NOMA) and orthogonal frequency division multiplexing (OFDM). Numerical results show that MMW-NOMA outperforms RP-NOMA and OFDM in throughput, mean square error, and energy efficiency. However, the complexity of MMW-NOMA is slightly higher than that of RP-NOMA but significantly lower than OFDM. These results show that MMW-NOMA achieves a reasonable trade-off between performance and complexity.

1. Introduction

An underwater acoustic network (UAN) is a monitoring system composed of sensor nodes with acoustic communication and computing capabilities [1]. They are widely used to discover marine resources, detect underwater life, monitor environmental conditions, predict tsunamis and underwater earthquakes, navigation, tracking, antitracking, torpedoes [2], etc. As common technologies of the OMA type, frequency division multiple access (FDMA), time division multiple access (TDMA), code division multiple access (CDMA), and orthogonal frequency division multiple access (OFDMA) allocate resources in the time, frequency, or code domains. According to OMA-based UANs, each data stream corresponds to a single node in the code, time, or frequency resource block [3]. Hence, it cannot access multiple nodes simultaneously within a limited spectrum.

As an emerging technology, NOMA consists of a power domain (PD-NOMA) [4] and a code domain (CD-NOMA) [5]. For PD-NOMA, the number of nodes is superimposed on the power domain to achieve multiplexing gain [6]. In NOMA-based UANs, signals are multiplexed in frequency and differentiated by the transmit power of the sender. Serial interference cancellation (SIC) resolves the signal with

different channel gains at the receiver [7]. Therefore, many nodes share the same resource block to ensure maximum transmission rate and fairness [8].

This paper proposes MMW-NOMA, an underwater uplink NOMA communication system. To the best of our knowledge, it is the first work to design a NOMA model based on maximum and minimum weight for underwater acoustic networks. The main contributions of the work are as follows.

First, we establish the MMW-NOMA model in a UAN scenario. Second, we design a node pairing algorithm based on maximum and minimum weight. Third, we design a node replacement mechanism by computing the channel correlation coefficient to learn more about the system. Furthermore, we suggest a power allocation method through distribution factors. Finally, we compare the performance of MMW-NOMA with that of randomly paired NOMA (RP-NOMA) and OFDM.

The rest of the paper is organized as follows. Section 2 introduces related work. Section 3 describes the implementation of the system. Section 4 shows the numerical results. Finally, Section 5 concludes this paper.

2. Related Work

2.1. Progress of NOMA-Based UANs. Recently, underwater NOMA technology has progressed considerably. Makled et al. [9] advice on a UAN with NOMA-based timing and frequency sharing mechanism for uplink and downlink information transmission. The results show that under the actual SIC algorithm, the sum rate of the network is higher than that of the OFDM-driven system. Wang and Qin [10] examine the spectral efficiency of underwater networks by modeling multiuser interference as a noncooperative game. Goutham and Harigovindan [11] present NOMA-CRS, a cooperative relay strategy-based NOMA for underwater acoustic networks. Experiments show that it significantly improves traversal and rate and energy efficiency.

Bocus et al. [12] study the performance of underwater NOMA systems using OFDM (NOMA-OFDM) and filter bank multicarrier (NOMA-FBMC). The results show that NOMA-FBMC has a higher bit rate. Jiang et al. [13] consider a partially overlapping NOMA algorithm (PO-NOMA) for the uplink UANs, which solves the optimal power allocation and determines the closed power spectral density (PSD). Esmaiel et al. [14] apply the time-reversed NOMA to mitigate the time-frequency dispersion of the underwater acoustic channel. Experiments show a higher bit error rate (BER) and outage probability than traditional methods. Goutham and Harigovindan [15] develop a full-duplex cooperative relay solution for a NOMA system (FD-CR-NOMA). The simulation results show that it significantly improves the ergodic rate, the probability of outage, and the energy efficiency of the UAN. Cheon and Cho [16] introduce a NOMA-based power allocation strategy for underwater acoustic networks. As a result of the numerical results, the proposed system improves performance over the sum-rate maximization (SRM) method. Liu et al. [17] design a NOMA scheme for large underwater systems. The experimental results show that the outage probability is low, and the spectral efficiency is high.

2.2. Advances in NOMA Node Pairing Strategies. Nodes share the same time or frequency resources in a NOMA uplink system and transfer data to base stations (BSs) with different transmit power. With the aid of SIC, the BS separates and decodes the multiplexed signal [18]. Therefore, node pairing and power distribution are fundamental components of the NOMA system.

Chen et al. [19] provide a pairing algorithm for massive MIMO-NOMA systems. It maintains the maximum sum rate by choosing one primary and one secondary for each pair. Theoretical analysis and simulation show that the algorithm has a lower interruption probability and higher sum rate. Mounchili and Hamouda [20] recommend a user pairing algorithm to ensure an optimal sum rate between NOMA clusters and improve performance with minimal gain differences. Salehi et al. [21] establish a collaborative NOMA (C-NOMA) system that allocates resources to maximize efficiency by using a user pairing scheme. Near-end users act as relays for maximum and minimum throughput. Numerical analysis shows that the average throughput of the C-NOMA system is better than that of the hybrid NOMA/OMA approach, while the fairness index decreases slightly. Wang et al. [22] present a positioning-based pairing scheme for MIMO-NOMA systems. The results show that the system reduces resource requirements and improves both time and frequency utilization.

2.3. NOMA-Based Power Allocation Technologies. Azam et al. [23] analyze the impact of power allocation in NOMA uplink systems. Experiments show that it maximizes the capacity of the uplink NOMA system while satisfying the individual rates for each user pair. Nguyen and Le [24] study a NOMA-based wireless network power allocation algorithm. Numerical results show that the performance is close to the optimal solution. Pischella and Ruyet [25] recommend a resource block allocation schema for PD-NOMA, which constructs resource blocks using the maximum weight matching strategy. Zuo and Tao [26] formulate the problem of maximizing throughput within the transmit power constraints of NOMA uplink systems. According to numerical results, it provides better throughput than its OMA counterpart.

Li et al. [27] present a power allocation algorithm in a MIMO-NOMA system using the Stackelberg game model, where the throughput of a single user is the optimization object. The optimal solutions for users and base stations are determined based on the Lagrangian multiplier scheme. The results show that energy consumption is reduced, and capacity is increased. Hao et al. [28] suggest a power allocation strategy for a multicarrier NOMA system based on an improved particle swarm optimization algorithm. The results show that the algorithm significantly improves energy efficiency. Zeng et al. [29] integrate NOMA into the OMA system to create an efficient allocation mechanism that treats users and resource blocks as bipartite graphs. By exchanging resources, they achieved a joint user-resource block. The numerical results show that the algorithm is more efficient than the OMA-based scheme. Jing et al. [30] propose a power allocation algorithm for the uplink Internet

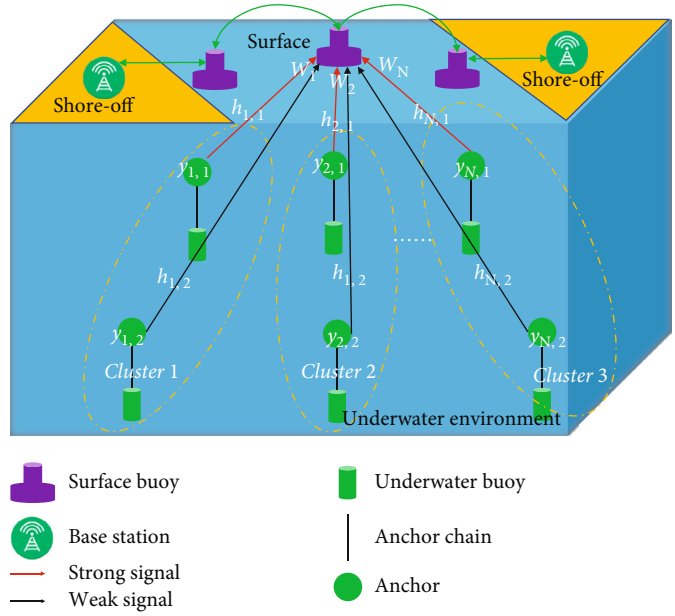

Figure 1: The MMW-NOMA model in the UAN scenario.

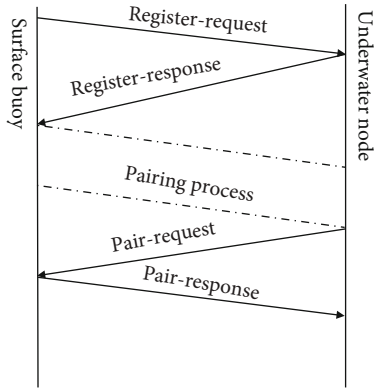

Figure 2: The node pairing procedure.

of Things (IoT) to maximize the traversal rate. Each node determines the transmitting power through feedback from the base station and a self-maintaining virtual queue. An experiment shows that the optimal power is obtained by comparing the queue length with traversal rate and using a low complexity dichotomy. Zeng et al. [31] introduce a dynamic power allocation algorithm to ensure the quality of service (QoS) in uplink NOMA systems. The simulation shows that it significantly improves energy efficiency and capacity.

3. The MMW-NOMA Communication System

3.1. The Uplink MMW-NOMA Model in a UAN Scenario. There are three main components in a UAN, namely, underwater nodes, surface buoys, and offshore buoy stations. All nodes are connected to an underwater buoy. Various sensors seal underwater buoy, and an anchor chain connects it to the anchor. When the node is deployed, the anchor chain sinks to the bottom, and the anchor chain expands to a fixed length depending on the application and location. All buoys are suspended in the water, forming a 3D structure. Surface buoys are located on autonomous underwater vehicles (AUVs), unmanned underwater vehicles (UUVs), remotely controlled vehicles (ROVs), and other devices that communicate between underwater nodes and offshore buoys.

For the MMW-NOMA uplink system, clusters are formed according to the region managed by the surface buoys. Each underwater node is considered a user. A near-end node (NEN) and a far-end node (FEN) are allocated in a cluster. We assume that NENs and surface buoys have relatively short Euclidean distances and good channel conditions. And the distance between the surface buoy and the FEN is longer, and the channel condition is poor. All resources, such as time, frequency, and code, are shared between the two-node cluster. Users are divided into orthogonal frequency clusters to simplify serial interference cancellation. The NOMA mechanism is running in intracluster communication, and the OMA technology is used in intercluster communication. Figure 1 shows the MMW-NOMA model in the UAN scenario.

In the MMW-NOMA system, the channels have different characteristics, and the node with good channel gain has the optimal power. The signals are sent simultaneously by some nodes whose strength is not correlated. The surface buoy receives all superimposed signals. Intracluster interference measured at underwater nodes is a function of channel gain. Therefore, nodes with low channel gain are more susceptible to strong intracluster interference. A SIC receiver mounted on a surface buoy decodes the signal, subtracts the interfering signal from the superimposed information, and resolves with a suboptimal gain. Subsequently, the signal is decoded.

For convenience, we designed an uplink MMW-NOMA scenario for a small-scale UAN. The underwater nodes are

transmitters in the system, and the surface buoy is the receiver. Each buoy has multiple antennas for sending and receiving. Supposing the number of underwater nodes is K ($K \geq 2n$). As a result, the received signal of the i-th cluster is shown as follows:

$$y_{i,j} = h_{i,j}\sum w_i x_i + n_{i,j}\, j = 1, 2, \tag{1}$$

where $h_{i,j}$ represents the channel vectors of the i-th cluster. $n_{i,j}$ means the white Gaussian noise. w_i is the i-th beamforming vector. x_i is the transmitting signal of the i-th set, which is expressed as follows:

$$x_i = \sqrt{\alpha_{i,1}} S_{i,1} + \sqrt{\alpha_{i,2}} S_{i,2}. \tag{2}$$

$S_{i,1}$ and $S_{i,2}$ are signals of a NEN and a FEN in the i-th cluster. $\alpha_{i,1}$ and $\alpha_{i,2}$ are the power factors of the two nodes, namely, $\alpha_{i,1} + \alpha_{i,2} = 1$. The channel matrix H is shown in the following equation:

$$H = \left[h_{1,1}^T, h_{2,1}^T, , h_{i,1}^T\right]^T, \tag{3}$$

where $[]^T$ is the transpose matrix, and $h_{i,1}$ is the channel vector of the NEN. The coding matrix is shown in the following equation:

$$W = [w_1, w_2, \cdots, w_i] = (H)^+ = (H)^*((H)(H)^*)^{-1}, \tag{4}$$

where w_i represents the zero-force beamforming (ZFBF) vector, $()^+$ is the pseudoinverse matrix, and $()^*$ is the conjugate complex number. Therefore, the signal which received by the NEN is shown in the following equation:

$$y_{i,1} = h_{i,1} w_i x_i + h_{i,1} \sum_{k=1}, k \neq n^N w_k x_k + n_{i,1} = h_{i,1} w_i \left(\sqrt{\alpha_{i,1}} S_{i,1} + \sqrt{\alpha_{i,2}} S_{i,2}\right) + h_{i,1} \sum_{k=1}, k \neq n^N w_k x_k + n_{i,1}, \tag{5}$$

where $h_{i,1}\sum_{k=1,k\neq n}^{N} w_k x_k$ is the signal interference. Since the NEN generates the beam forming vector, it can be eliminated by ZFBF. Thus, we get that $h_{i,1} w_k = 0, k \neq n$. $h_{i,1} w_i(\sqrt{1-\alpha_i} S_{i,2})$ is the interference of a FEN, which can be eliminated by a SIC receiver, so the received signal of the NEN is simplified, as shown in the following equation:

$$y_{i,1} = h_{i,1} w_i \left(\sqrt{\alpha_{i,1}} S_{i,1}\right) + n_{i,1}. \tag{6}$$

Since SIC and ZFBF cannot be used to cancel interference of the FEN, the received signal of a FEN is shown in the following equation:

$$y_{i,2} = h_{i,2} w_i \left(\sqrt{\alpha_{i,1}} S_{i,1} + \sqrt{\alpha_{i,2}} S_{i,2}\right) + h_{i,2} \sum_{k=1}, k \neq n^N w_k x_k + n_{i,2}. \tag{7}$$

3.2. The Node Pairing Algorithm. After the UAN is deployed, the surface buoy broadcasts a register-request message. The underwater node responds to the buoy with a register-response message. After decoding the register-response message containing the node ID, location, energy, and signal strength, the surface buoy resolves the pairing weight and creates a weight table. Then, the underwater node sends a pair-request message. The buoy checks the weight table and responds with a pair-response message. Figure 2 shows the pairing procedure.

This paper suggests a maximum and minimum weight algorithm to construct the node pairing procedure. Two nodes with considerable differences in gain are paired into a cluster and share the same channel resources. The NEN is the closest node to the surface buoy and has optimal channel conditions. The FEN is relatively far from the surface buoy, and the channel conditions may be poor. The pairing weight may be the same when considering position and residual energy. In this case, the node with the smallest ID will be selected first.

An objective of the pairing algorithm is to establish a hierarchical weight difference between a FEN and a NEN. As shown in (8), the nodes must meet the maximum pairing weight.

$$\text{Pair}\langle N_{\text{Near}}, N_{\text{Far}}\rangle = \arg \max_{n_1 \in \cup_{\text{Near}} n_2 \in \cup_{\text{Far}}} (\psi_{\text{NOMA}}), \tag{8}$$

where N_{Near} and N_{Far} mean the FEN and the NEN. $\cup_{\text{Near}}$ and $\cup_{\text{Far}}$ are sets of NENs and FEN, respectively. The pairing weight $\psi(i)_{\text{NOMA}}$ is shown in the following equation:

$$\psi(i)_{\text{NOMA}} = \sum_{i=1}^{n} \frac{\lambda_i S_i}{\eta_i L_i}, \tag{9}$$

where λ_i is the factor of the residual energy for node i, S_i is the signal strength, η_i is the distance factor, and L_i is the Euler distance between node i and the surface buoy. Algorithm 1 shows the node pairing algorithm.

Algorithm 1 description: this program implements the node pairing process of MMW-NOMA. Pair generation is established based on node state values in the traversal system. The remaining energy and distance factor are inputs to the program. The pairing weights for nodes are calculated based on their Euclidean distance from the buoy. Then, implement the mapping between nodes and their pairing factors and construct a max weight queue and min weight queue. It constructs the min-max node pair by selecting each queue object.

Procedure $Node_{pair}()$
Input: λ, η
//input the residual energy factor, distance factor
For (i **=0;** i **<20;** i**++)** {
  $L_i \longleftarrow L(i, \mathrm{B})$
    //calculate the Euclidean distance between node i and buoy B
  $\psi(i)_{NOMA} \longleftarrow \sum_{i=1}^{n} (\lambda S/\eta L_i)$
    //compute the pairing weight of node i
  Map.Add($\psi(i)_{NOMA}$, i);
    //map node i and the corresponding pair weight ψ
  }
End for
  keyVlaues = **map.getKeys**();
    //calculate the weights of all mapped nodes;
  Sort(keyVlaues);
      //order the node weight
  m =0
    //the pointer points to the minimum weight of the node
  n = arr.Length − 1
    //the pointer points to the maximum weight of the node
While (m < n) **do**
  {
  Max = map.getValues(keyVlaues[n])
    //get the node of maximum weight
  Min = map.getValues(keyVlaues[m])
      //get node of minimum weight
  Nodes.Add($Pair\langle N_{\max}, \mathrm{N}_{\min}\rangle$)//add a node pair
  m++
    //move the pointer to the second smallest weight
  n–
    //move the pointer to the next highest weight
  }
End while
Output: $Pair\langle N_{\max}, \mathrm{N}_{\min}\rangle$ //output the paired node pair nodes
End procedure

Algorithm 1: The maximum and minimum weight-based pairing algorithm.

3.3. The Node Replacement Schema. The nodes move due to ocean currents. Thus, the distance between the NEN, FEN, and the surface buoy can vary. Furthermore, the energy of each node must be consumed. Therefore, a node replacement mechanism must be designed. We define a relevant threshold τ based on business requirements during initialization. After a period of operation, the node sends its channel status message (CSI) to the surface buoy. The buoy uses CSI to calculate the channel correlation coefficient between two nodes, as shown in the following equation:

$$\mathrm{Corr}\left(\mathrm{NEN}_i, \mathrm{FEN}_j\right) = \frac{\left|h_i \cdot h_j\right|}{\left|h_i\right|\left|h_j\right|} > \tau. \tag{10}$$

If $\mathrm{Corr}(\mathrm{NEN}_i, \mathrm{FEN}_j) > \tau$, the buoy will count for the gain difference between the NEN and the FEN and then store it in Ch_{Diff}, which is the set of gain difference, as shown in the following equation:

$$Ch_{\mathrm{Diff}} = \left\{D_{\mathrm{gain}}\left(\mathrm{NEN}_i, \mathrm{FEN}_j\right) = \left|\left|h_i\right| - \left|h_j\right|\right|\right\}, \tag{11}$$

where $D_{\mathrm{gain}}(\mathrm{NEN}_i, \mathrm{FEN}_j)$ is the gain difference between a NEN and a FEN.

After that, the surface buoy traverses unpaired nodes in the UAN and calculates their peak signal-to-noise ratio (PSNR) in turns. The buoy selects a node x with the largest PSNR and compares it with node j. If $\mathrm{PSNR}_{\max\,(x)} > \mathrm{PSNR}_{\mathrm{FEN}(j)}$, it will use node x to replace node j, as shown in the following equation:

$$\mathrm{Pair}_{\mathrm{new}} = \mathrm{Pair}\langle \mathrm{NEN}_i, x\rangle = \arg\max \left\{D_{\mathrm{gain}}(\mathrm{NEN}_i, x)\right\}. \tag{12}$$

If $\mathrm{PSNR}_{\max\,(x)} \le \mathrm{PSNR}_{\mathrm{FEN}(j)}$, it maintains the pairing of NEN_i and FEN_j, as shown in the following equation:

$$\mathrm{Pair}_{\mathrm{new}} = \mathrm{Pair}\left\langle \mathrm{NEN}_i, \mathrm{FEN}_j\right\rangle = \arg\max \left\{D_{\mathrm{gain}}\left(\mathrm{NEN}_i, \mathrm{FEN}_j\right)\right\}. \tag{13}$$

Algorithm 2 shows the node replacement mechanism.

Algorithm 2 description: this program implements the node replacement mechanism. The channel correlation

Procedure $Node_{displace}()$
Input: τ //input the channel correlation threshold
For(i =0; i <20; i++)
{
For(j =20; j >0; j–)
{
$Corr(i, j) \longleftarrow |h_i \cdot h_j|/|h_i||h_j|$ //count for the channel correlation
$Ch_{Diff} \longleftarrow ||h_i| - |h_j||$ //count for the channel gain difference set
}
If($PSNR_{\max(x)} > PSNR_{FEN(j)}$){
$Pair_{New} \longleftarrow Pair\langle NEN_i, x\rangle$ //replace FEN_j with node x
$Pair\langle NEN_i, x\rangle \longleftarrow \arg\max\{D_{gain}(NEN_i, x)\}$
//modify channel gain difference
}
Else
{
$Pair_{New} \longleftarrow Pair\langle NEN_i, NEN_j\rangle$//keep the initial node pair
}
Output:$Pair_{New}$;
}
End procedure

Algorithm 2: The node replacement algorithm.

Procedure $P_{Allcation}()$
Input: P_{sum}, R_{th}
//input the maximum transmit power and communication threshold
For(i =0; i <20; i++)
{
$MSE_{NOMA} \longleftarrow \sum_{i=1}^{2}\alpha_i + (\beta_i/r_i + c_i)$; //count for MSE of NOMA
$MSE_{OMA} \longleftarrow \sum_{i=1}^{2}a_i + (b_i/0.5r_i + c_i)$; //count for the MSE of OMA
$f(\alpha_i) \longleftarrow MSE_{i,1} + MSE_{i,2}$; //solve the NOMA objective function
$g(\alpha_i) \longleftarrow MSE_{i,1} + MSE_{i,2} - MSE_{OMA}$;
//solve NOMA constraint
$\mu_2 \longleftarrow [(2^{R_{th}}\text{-}1/\gamma h_2), (h_1\text{-}\xi/h_1 + h_2)]$; //solve power distribution factor
}
Output: P_2,$P_1 \longleftarrow P_{sum} - P_2$;
End procedure

Algorithm 3: The power allocation algorithm.

threshold τ is an input to the program. The channel correlation coefficient and channel gain difference are counted by traverse nodes of the MMW-NOMA system. The buoy selects the node x with the peak signal-to-noise ratio (PSNR) in turns and compares it with node j. If it is greater than j, replace j with x, and modify the channel gain, otherwise, maintain the original node pair.

3.4. The Power Allocation Mechanism. Once the pairing procedure is complete, MMW-NOMA communication will be implemented in each cluster. Therefore, a power distribution mechanism for the FEN and the NEN should be devised. The achievable data rate reflects the capacity of each node. The mean square error (MSE) of NOMA is shown in the following equation:

$$\mathrm{MSE}_{\mathrm{NOMA}} = \sum_{i=1}^{2}\alpha_i + \frac{\beta_i}{r_i + c_i}, \tag{14}$$

where α, β, and c indicate the transmission coefficients, and r denotes the transmission rate. Unlike the OMA mode, which needs two slots to support n nodes, the MMW-NOMA system requires only a slot to supply them. Consequently, the data transmission rate is half that of the NOMA

model, as shown in the following equation:

$$\mathrm{MSE}_{\mathrm{OMA}} = \sum_{i=1}^{2} a_i + \frac{b_i}{0.5r_i + c_i}. \tag{15}$$

The optimization of power allocation in MMW-NOMA

The objective function $f(\alpha_i)$ and the restrictive condition is shown in the following equation:

$$[\alpha_i] = \arg\min \{f(\alpha_i)\}, \quad s.t\ g(\alpha_i) \le 0 \quad h(\alpha_i) = 0, \tag{16}$$

As the optimal solution, α_i is derived by the Karush-Kuhn-Tucker (KKT) condition, as shown in the following equation:

Let $\gamma = P_{\mathrm{sum}}/N_0$, the transmission rates of a NEN and a

$$\begin{cases} \dfrac{\partial f(\alpha_i)}{\partial \alpha_i} + \sum_{j=1}^{m} \mu_j \dfrac{\partial g(\alpha_i)}{\partial \alpha_i} + \sum_{k=1}^{l} \lambda \dfrac{\partial h_k}{\partial \alpha_i} = 0, (i = 1, 2, \cdots, n), h_k(\alpha_i) = 0, (k = 1, 2, \cdots, l), \mu_j g(\alpha_i) = 0, (j = 1, 2, \cdots, m), \mu_j \ge 0. \end{cases} \tag{17}$$

$g(\alpha_i)$ are derived by KKT, as shown in the following equations, respectively.

$$\frac{f(\alpha_i) = \mathrm{MSE}_{i,1} + \mathrm{MSE}_{i,2} = a_1 + b_1}{\frac{r_1 + c_1 + a_2 + b_2}{r_2 + c_2},} \tag{18}$$

$$g(\alpha_i) = \mathrm{MSE}_{i,1} + \mathrm{MSE}_{i,2} - \mathrm{MSE}_{\mathrm{OMA}}, \tag{19}$$

where $\mathrm{MSE}_{\mathrm{OMA}}$ represents the MSE in the quadrature modulation mode.

Consider a cluster with a FEN and an NEN, and suppose that the channel condition of the NEN is better than the FEN, i.e., $h_1 > h_2$. Consequently, the transmission rates are shown in the following equation:

$$r_1 = \log_2\left(\frac{1 + P_1 h_1}{P_2 h_2 + N_0}\right), r_2 = \log_2\left(\frac{1 + P_2 h_2}{N_0}\right), \tag{20}$$

where P_1 and P_2 are the transmit power of the NEN and FEN, and N_0 is the Gaussian white noise.

Due to the decoding order, NEN first performs signal parsing on the buoy using the SIC mechanism. However, NENs interfere with FENs. When a NEN signal decodes, it subtracts from FEN signal, and then, the FEN signal is decoded. The power allocation factors are shown in the following equation:

$$\frac{\frac{\mu_1 = P_1}{P_{\mathrm{sum}}}, \mu_2 = P_2}{P_{\mathrm{sum}},} \tag{21}$$

where $\mu_1 + \mu_2 = 1$, P_{sum} means the transmitting power of the cluster, that is, $P_{\mathrm{sum}} = P_1 + P_2$.

FEN are shown in the following equation:

$$r_1 = \log_2\left(\frac{1 + \gamma\mu_1 h_1}{\gamma\mu_2 h_2 + 1}\right), r_2 = \log_2(1 + \gamma\mu_2 h_2). \tag{22}$$

The throughput of the nodes pair may be counted by adding the transmission rates, as shown in the following equation:

$$r_{\mathrm{sum}} = \log_2(1 + \gamma\mu_1 h_1 + \gamma\mu_2 h_2) = \log_2((1 + \gamma\mu_2(h_2 - h_1) + \gamma\mu_1 h_1)). \tag{23}$$

For an MMW-NOMA system, there is a limit to the power allocated to the node with optimal channel gain. When the surface buoy demodulates the received signal, there is a power interval ΔP between a NEN and FEN, which can ultimately be used to determine the maximum transmission power of the NEN and the FEN. The constraints of ΔP are shown in the following equation:

$$P_2 h_2 - P_1 h_1 \ge \Delta P. \tag{24}$$

Based on (24), the power allocation factors μ_1 and μ_2 can be rewritten as the following equation:

$$\mu_1 h_1 - \mu_2 h_2 \ge \xi, \tag{25}$$

where $\xi = \Delta P/P_{\mathrm{sum}}$, so the upper limit of the power allocation factor is shown in the following equation:

$$\frac{\mu_2 \le h_1\text{-}\xi}{h_1 + h_2.} \tag{26}$$

Let R_{th} be the communication threshold of FEN, and $r_2 > R_{\mathrm{th}}$ be a condition to maintain the normal communication. Then, we obtain the lower limit of the power allocation

Table 1: Experimental parameters.

Parameter	Value
Channel type	Rayleigh fading
Noise type	Complex Gaussian
Statistical methods	Monte Carlo
Carrier frequency	15 kHz
Sampling rate	24 kbps
Symbol rate	244
Queue size	1024
Number of frames	128
Impulse response of UAC	45 dB
Channel bandwidth	6 kHz
Distance of NEN	1-300 m
Distance of FEN	300-800 m
Doppler spread factor	0.3-1.4
Maximum multipath delay	40 ms
Absorption coefficient	4
Residual energy threshold	0.35
Delay threshold	0.01
BER threshold	0.005

factor, as shown in the following equation:

$$\frac{\mu_2 \geq 2^{R_{\text{th}}}\text{-}1}{\gamma h_2.} \tag{27}$$

Algorithm 3 shows the power allocation algorithm.

Algorithm 3 description: this program is used to implement the power distribution of the MMW-NOMA system. The maximum transmit power and communication threshold are inputs to the program. First, traverse whole nodes to count the MSE of the NOMA system and then compute the MSE in the OMA type. Followed by, solving the objective function and constraint value of the NOMA system, and calculate the power distribution factor of the FEN node and NEN node.

4. Numerical Results

4.1. Experimental Settings. We set up an experiment with a surface buoy and 20 underwater nodes in an underwater MMW-NOMA scenario. The buoy is fixed with 48 hydrophones, and each underwater node has two hydrophones. The Poisson distribution is considered to be the system deployment model. Typically, nodes are 3 to 10 meters deep. Various tools are used in this experiment, including MATLAB 2019, WOSS, and BELLHOP Acoustic Toolbox [32]. The following main parameters are listed in Table 1.

Suppose that the acoustic channel is perfectly known and that the underwater nodes are divided into ten clusters based on the pairing algorithm. The OFDM technology is used for intracluster communication, and NOMA is used for intercluster communication. We compare MMW-NOMA with RP-NOMA and OFDM techniques in exact scenarios. For a RP-NOMA communication system, clusters are formed via the random pairing mechanism. In OFDM, all nodes are considered a management cluster. Specifically, throughput, MSE, energy efficiency, and complexity of the three systems are compared. We design an MMW-NOMA simulation program. Figure 3 shows the distribution plots for 20, 40, 80, and 160 node pairs.

4.2. Comparison of Throughput. In general, throughput refers to the amount of data successfully transmitted per cycle and is an essential indicator of a communication system. This work evaluates the achievable throughput of MMW-NOMA, RP-NOMA, and OFDM. The performance of the three methods at different nodes is shown in Figure 4. The cumulative distribution function (CDF) of throughput is shown in Figure 5.

Under low SNR conditions, MMW-NOMA shows roughly the same throughput as RP-NOMA. As SNR increases, MMW-NOMA outperforms RP-NOMA, while OFDM has relatively low throughput. Simulation results show that MMW-NOMA has specific advantages in terms of high throughput with multiple nodes.

A pair of nodes is scheduled simultaneously for each subband in MMW-NOMA. In addition to the near- and far-reaching effect, the SIC receiver is also used to decode and demodulate the signal. Therefore, we choose more levels of modulation and coding strategy (MCS) for the allocation of power to underwater nodes. However, the possibility of selecting the MCS level in the OFDM scheme is low, which undoubtedly leads to low throughput. MMW-NOMA uses maximum and minimum weight to reduce correlation and interference and maintain optimal throughput. As for RP-NOMA, it uses the random pairing algorithm between nodes, and the channel difference between a FEN and a NEN cannot be kept optimally unchanged. Therefore, throughput of RP-NOMA is lower than that of MMW-NOMA. Overall, it achieves the minimum transfer rate and SIC constraints in MMW-NOMA and improves signal and throughput.

4.3. Performance of the MSE. Measurement of MSE is critical to determining the reliability of a communication system. The MSE of a UAN refers to both the propagation characteristics of the underwater channel and the access technology. This paper compares the MSEs of MMW-NOMA, RP-NOMA, and OFDM without channel coding. The MSEs with different numbers of nodes are shown in Figure 6. As the number of nodes increases, the MSE of all three systems increases. In contrast, the rise of OFDM is enormous. Furthermore, the MSEs of RP-NOMA and MMW-NOMA are approximately the same.

Figure 7 illustrates the MSE at different SNRs. It is clear that as the SNR increases, the MSE of the three systems decreases. In contrast, the MSE of OFDM is relatively high, while the MSE of MMW-NOMA is slightly lower. MMW-NOMA shows the most significant reduction in MSE.

Due to the fixed modulation strategies in OFDM, the MSE is determined by the subcarrier that performs the most poorly. However, the multiplexed signal is less sensitive to the delay of channel-dependent feedback in MMW-NOMA,

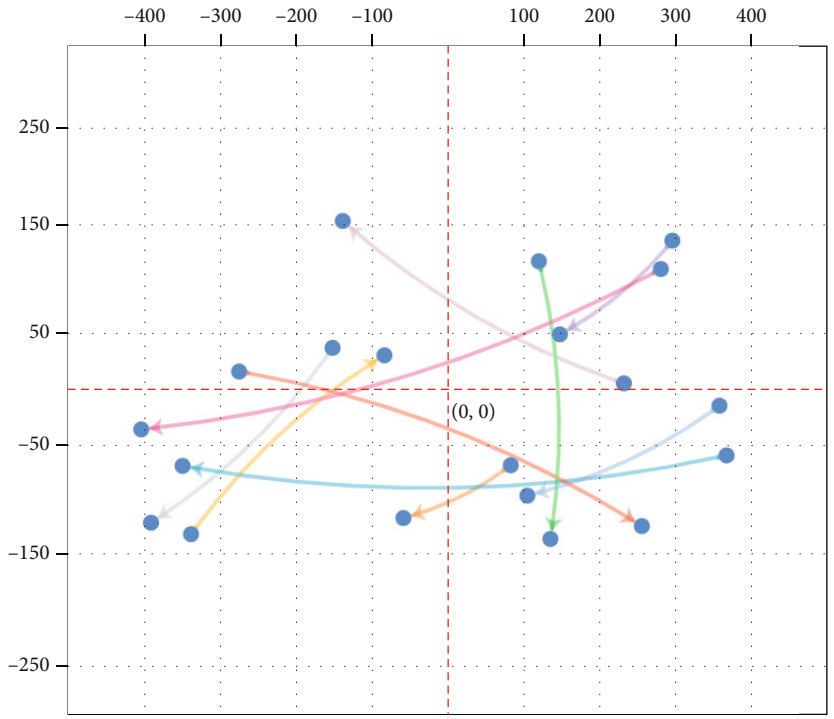

(a) Pairing of 20 nodes

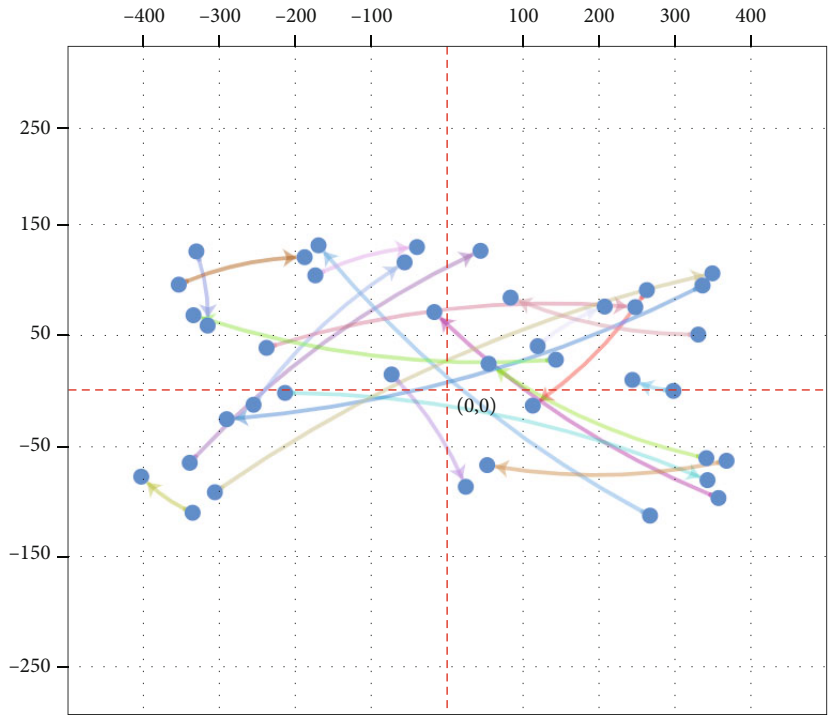

(b) Pairing of 40 nodes

Figure 3: Continued.

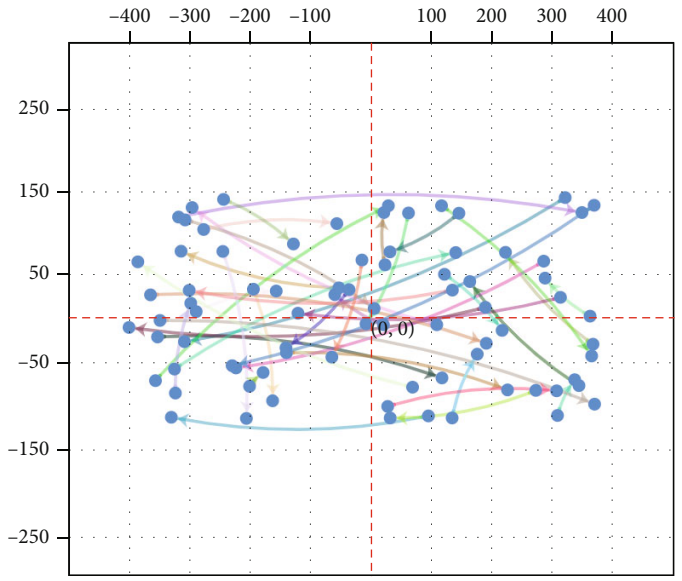

(c) Pairing of 80 nodes

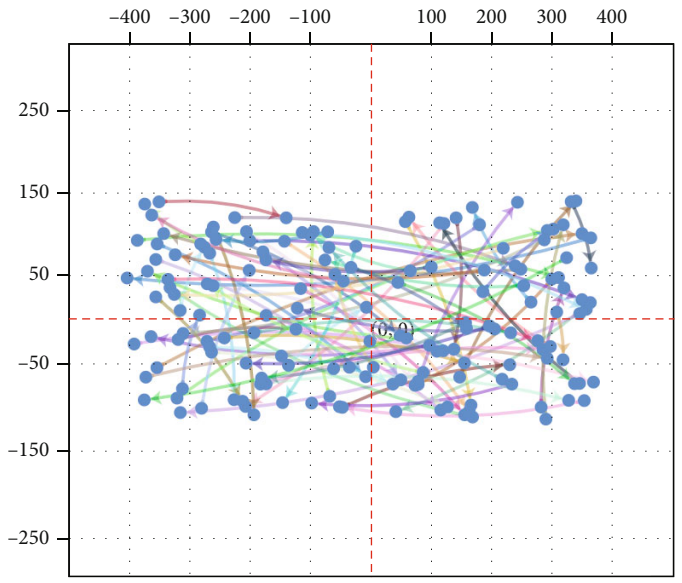

(d) Pairing of 160 nodes

Figure 3: The distribution diagrams of node pairs in MMW-NOMA.

or CSI no longer strongly affects the multiplexed signal. A significant difference between MMW-NOMA and RP-NOMA is that the optimal gain difference of a NEN and FEN is not fully guaranteed. If the gain difference is slight, the throughput will be reduced. Therefore, the MSE of RP-NOMA is higher than that of MMW-NOMA.

4.4. Comparison of Energy Efficiency. In general, batteries power underwater nodes with limited energy. It is difficult to replace the battery or charge it after deploying a node. Since the UAN is an energy-constrained system, energy efficiency is a crucial factor to consider. Figure 8 shows the energy efficiency for MMW-NOMA, RP-NOMA, and OFDM with different transmitting power. As the transmission power increases, the energy efficiency of the three systems increases. In contrast, the energy efficiency of MMW-NOMA is approximately 13.33% higher than that of OFDM and 4.31% higher than that of RP-NOMA.

Figure 9 illustrates the EE of three systems with different transmission rates. For MMW-NOMA, it uses the maximum and minimum weight algorithm to achieve the optimal fair distribution of FENs and NENs and then constructs a power control strategy based on the allocation factor to optimize energy efficiency. Although RP-NOMA adopts the power control schema based on NOMA, there is no suitable node replacement mechanism. FENs and NENs cannot be

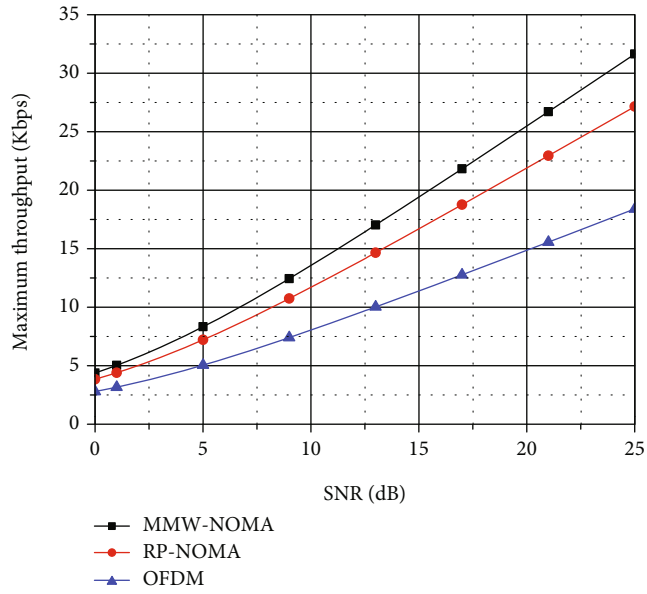

Figure 4: Throughput vs. SNR.

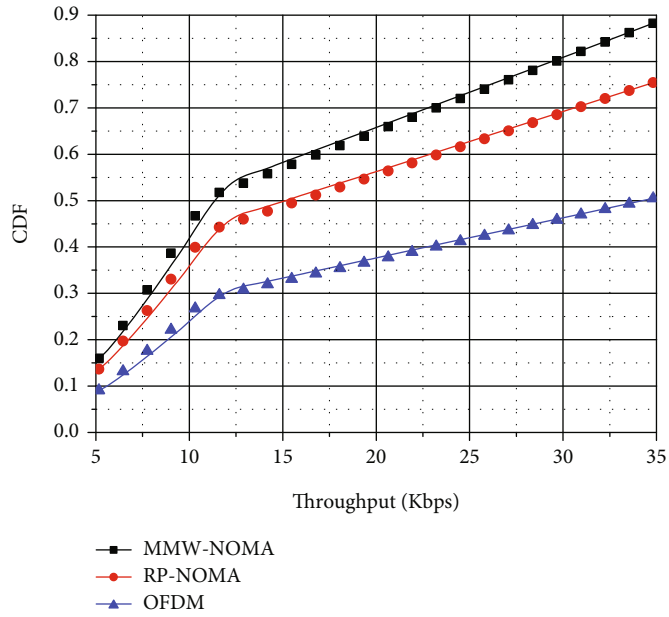

Figure 5: CDF vs. throughput.

allocated fairly and optimally using a random pairing algorithm. Therefore, the energy efficiency of RP-NOMA could not be significantly improved.

All three systems show a decreasing trend in energy efficiency as the transmission rate increases. Experiments show that the energy efficiency of NOMA is higher than that of OMA technology. NOMA allocates spectrum resources to multiple nodes and selects SIC at the receiver to maximize system capacity. On the contrary, OMA only grants resources to a single node and cannot be used at the receiving end, thus failing to reach maximum capacity.

4.5. Comparison of Complexity. Complexity is a crucial metric for evaluating the real-time performance of a communication system. When the number of nodes is less than 8, the complexity of the three methods is close to the same level, as shown in Figure 10. However, the complexity of OFDM increases significantly with the number of nodes, while that of MMW-NOMA is slightly higher than that of RP-NOMA.

The acoustic channel resources of underwater OFDM systems are limited, and subcarrier allocation is required to minimize the transmission power and maximum the transmission

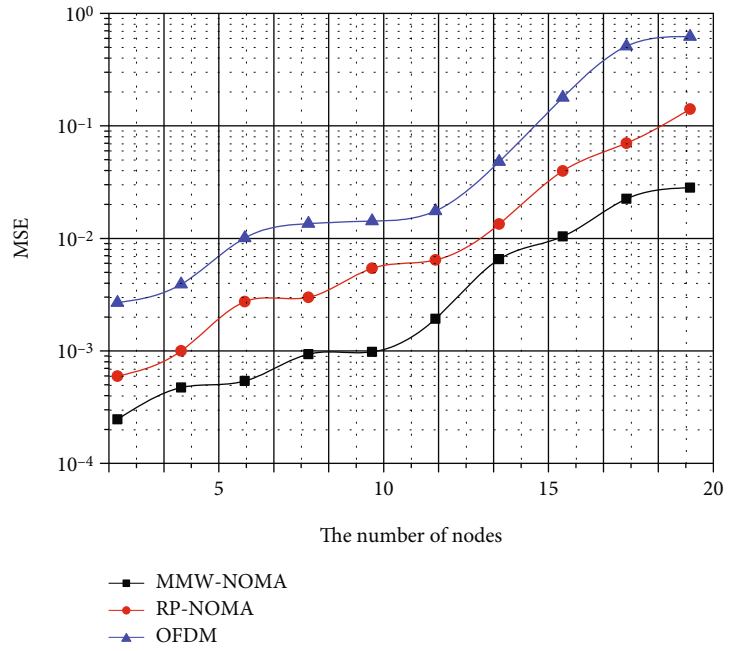

Figure 6: MSE vs. the number of nodes.

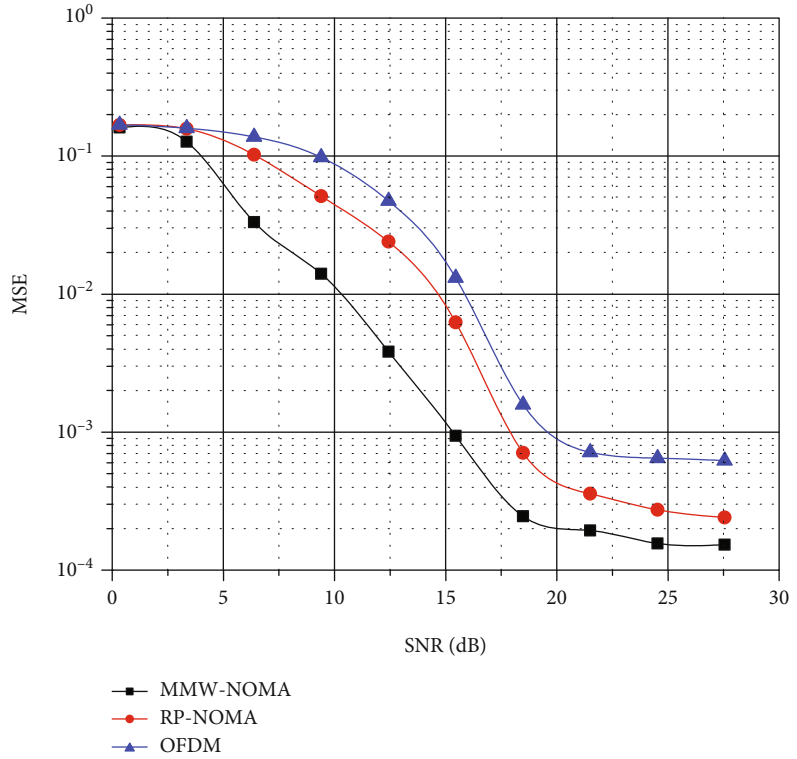

Figure 7: MSE vs. SNR.

rate. For an OFDM system, surface buoys allocate resources to each node based on CSI and associated subcarrier allocation criteria. When CSI changes, the buoy reassigns subcarriers. Therefore, the complexity of multiplication for subcarrier allocation and update reallocation is $O(n^3)$, and that of addition is $O(n)$ in an OFDM system with n nodes. For MMW-NOMA, the multiplicative complexity of node pairing, node selection, replacement, and power allocation is $O(n^2)$, and that of addition is $O(n/2)$. For RP-NOMA, the node pairing scheme is realized based on the random elimination mechanism. The

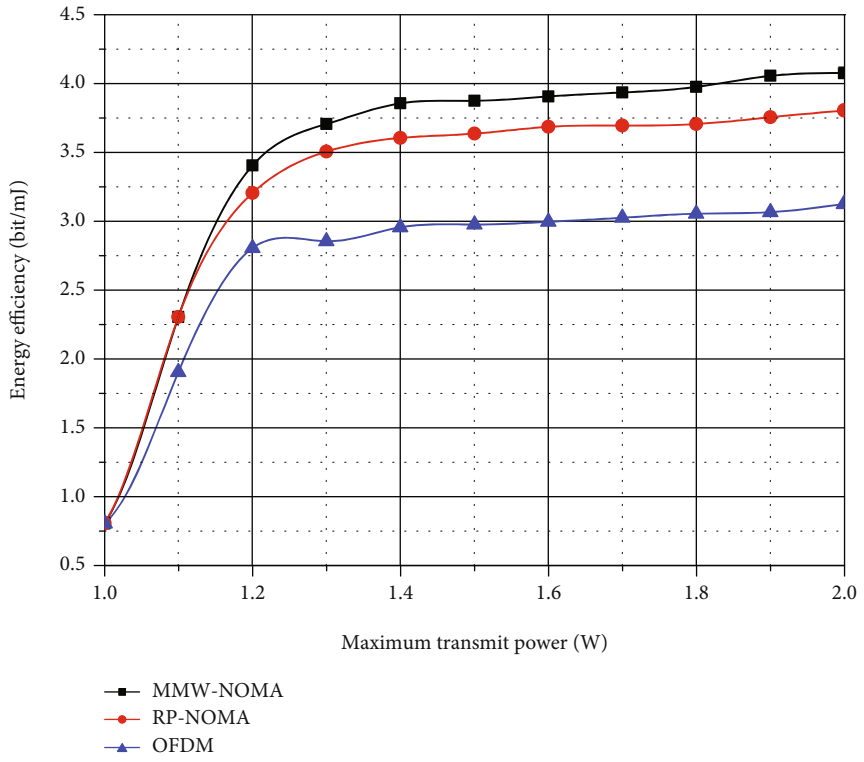

Figure 8: Energy efficiency vs. transmission power.

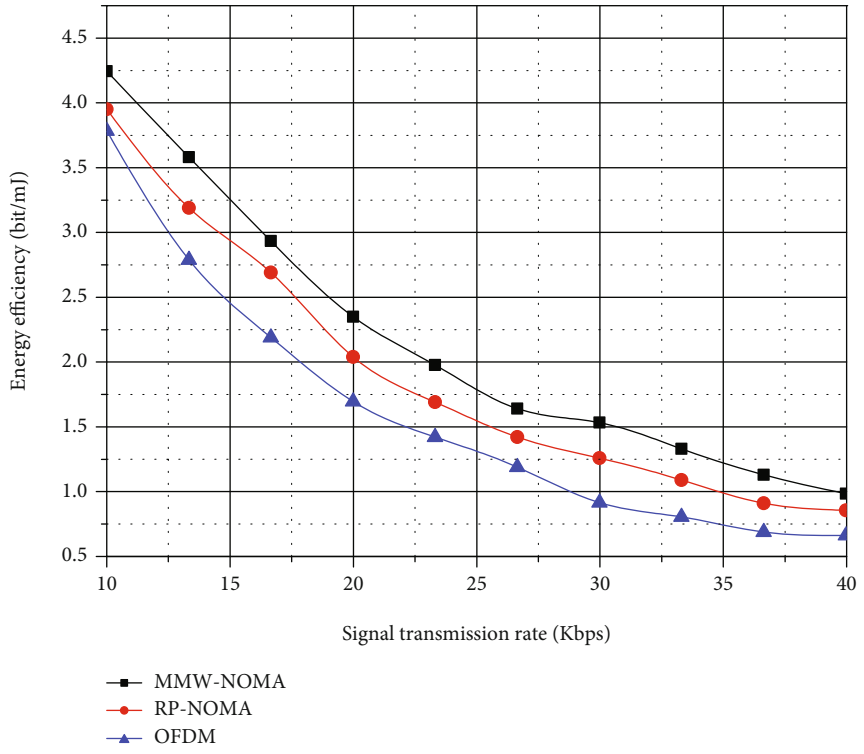

Figure 9: Energy efficiency versus transmission rates.

complexity of multiplication is $O(n^2/4)$, and that of addition is $O(n/2)$. Multiple clusters are constructed in MMW-NOMA and RP-NOMA, and OFDM communication is still used between clusters. Thus, the complexity of multiplication and addition is increased relative by $O(n^3/8)$ and $O(n/2)$, respectively, for MMW-NOMA and RP-NOMA.

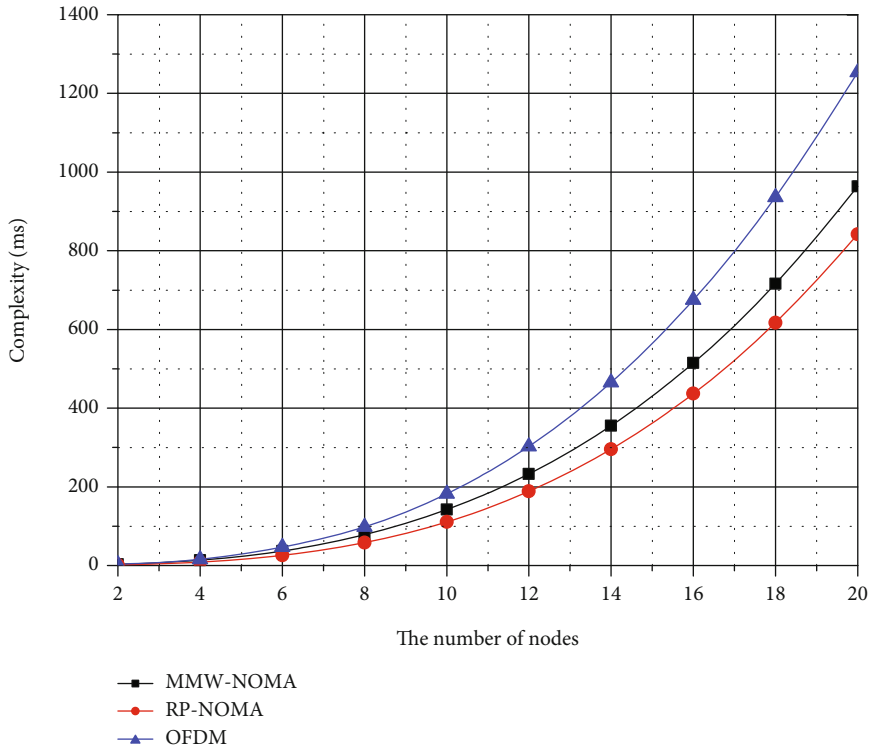

Figure 10: The complexity of the three systems.

5. Conclusions

This paper proposes MMW-NOMA, a NOMA communication system that allocates power to underwater nodes based on the quality of the channel. We build the MMW-NOMA model in the UAN scene. SIC receivers placed on surface buoys allow the superimposed signals to be separated from each other. These superimposed signals share the same time or frequency resource block. We design a node pairing algorithm based on maximum and minimum weight. To verify performance, we review the throughput, MSE, EE, and complexity of MMW-NOMA, RP-NOMA, and OFDM, respectively. The simulation shows that it achieves the highest throughput in MMW-NOMA, keeps the smallest MSE, and guarantees the highest EE. Nonetheless, under the same experimental scenario, the complexity is slightly higher than RP-NOMA, but significantly lower than that of OFDM. It has been shown that MMW-NOMA achieves a reasonable balance between performance and complexity.

As an interesting research direction, we are designing a prototype for a NOMA-enabled underwater node. Based on this work, we intend to verify the performance of MMW-NOMA in various scenarios thoroughly. Currently, we have designed a UAN [33–36] built on a software-defined networking (SDN) architecture. It is worth mentioning that the development process of UAN can be significantly shortened, and experimental construction can be easily realized based on SDN. Then, field deployment and small-scale experiments will be the main work.

Abbreviations

AUVs:	Autonomous underwater vehicles
BS:	Base station
BER:	Bit error rate
CSI:	Channel status message
CDMA:	Code division multiple access
CD-NOMA:	Code domain NOMA
C-NOMA:	Collaborative NOMA
CDF:	Cumulative distribution function
FEN:	Far-end node
FDMA:	Frequency division multiple access
FD-CR-NOMA:	Full-duplex cooperative relay for NOMA
IoT:	Internet of Things
KKT:	Karush-Kuhn-Tucker
MMW-NOMA:	Maximum and minimum weights-based NOMA
MSE:	Mean squared error
MIMO-NOMA:	Multiple in multiple out based NOMA
MCS:	Modulation and coding strategy
NEN:	Near-end node
NOMA-FBMC:	NOMA using filter bank multicarrier
NOMA-OFDM:	NOMA using OFDM
NOMA-CRS:	Cooperative relay-based NOMA
NOMA:	Nonorthogonal multiple access
OFDMA:	Orthogonal frequency division multiple access
OFDM:	Orthogonal frequency division multiplexing
OMA:	Orthogonal multiple access

PO-NOMA: Partially overlapping NOMA
PD-NOMA: Power domain NOMA
PSD: Power spectral density
QoS: Quality of service
RP-NOMA: Randomly paired NOMA
ROVs: Remotely controlled vehicles
RB: Resource block
SIC: Serial interference cancellation
SRM: Sum-rate maximization
TDMA: Time division multiple access
UAN: Underwater acoustic network
UUVs: Unmanned underwater vehicles
ZFBF: Zero-force beamforming.

Data Availability

The data used to support this study are available from the corresponding author upon request.

Conflicts of Interest

The authors declare that they have no conflicts of interest.

Acknowledgments

This work was supported in part by the Science and Technology Major Project of Xinxiang City under Grant 21ZD003, in part by the Key Scientific and Technological Project of Henan Province under Grant nos. 222102320181, 222102110011, 212102210422, 212102310087, and 202102210388, in part by the Young Scholar Training Program of Higher Education in Henan Province under Grant 2019GGJS172, and in part by the Key Scientific Research Project of Colleges and Universities in Henan Province under grant 20A520002 and 21A520001.

References

[1] S. Jiang, "On reliable data transfer in underwater acoustic networks: a survey from networking perspective," *IEEE Communications Surveys & Tutorials*, vol. 20, no. 2, pp. 1036–1055, 2018.

[2] H. Jin, B. Liu, and W. Chen, "Research on the nodes deployment scheme for sensor coverage in underwater wireless networks based on genetic algorithm," *Chinese Journal of Sensors and Actuators*, vol. 32, no. 7, pp. 1083–1087, 2019.

[3] J. Wu, Z. Zhang, and J. Wang, "Joint time and beam domain non-orthogonal multiple access," *Journal on Communications*, vol. 42, no. 4, pp. 76–88, 2021.

[4] T. Park, G. Lee, W. Saad, and M. Bennis, "Sum rate and reliability analysis for power-domain nonorthogonal multiple access (PD-NOMA)," *IEEE Internet of Things Journal*, vol. 8, no. 12, pp. 10160–10169, 2021.

[5] X. Yue, Y. Liu, Y. Yao, X. Li, R. Liu, and A. Nallanathan, "Secure communications in a unified non-orthogonal multiple access framework," *IEEE Transactions on Wireless Communications*, vol. 19, no. 3, pp. 2163–2178, 2020.

[6] Y. Sun, Y. Liu, J. Zhou, Q. Cao, and S. Li, "Sum-rate maximization in MIMO NOMA system with imperfect CSI," *Journal on Communications*, vol. 40, no. 11, pp. 94–100, 2019.

[7] O. Maraqa, A. S. Rajasekaran, S. Al-Ahmadi, H. Yanikomeroglu, and S. M. Sait, "A survey of rate-optimal power domain NOMA with enabling technologies of future wireless networks," *IEEE Communications Surveys & Tutorials*, vol. 22, no. 4, pp. 2192–2235, 2020.

[8] S. Hu, J. Zhang, Y. Lu, B. Liu, and J. Han, "Power control for successive interference cancellation algorithm based on game theory," *Journal on Communications*, vol. 36, no. 9, pp. 215–221, 2015.

[9] E. A. Makled, A. Yadav, O. A. Dobre, and R. D. Haynes, "Hierarchical full-duplex underwater acoustic network: a NOMA approach," in *OCEANS 2018 MTS/IEEE Charleston*, pp. 1–6, Charleston, SC, USA, October 2018.

[10] Z. Wang and F. Qin, "NOMA based efficient spectrum sharing for underwater UAV system with multi-agent reinforcement learning," in *International Conference on Industrial Artificial Intelligence (IAI)*, pp. 1–5, Shenyang, China, October 2020.

[11] V. Goutham and V. P. Harigovindan, "NOMA based cooperative relaying strategy for underwater acoustic sensor networks under imperfect SIC and imperfect CSI: a comprehensive analysis," *IEEE Access*, vol. 9, pp. 32857–32872, 2021.

[12] M. Bocus, D. Agrafiotis, and A. Doufexi, "Non-orthogonal multiple access (NOMA) for underwater acoustic communication," in *IEEE Vehicular Technology Conference (VTC-Fall)*, pp. 1–5, Chicago, IL, USA, August 2018.

[13] Z. Jiang, X. Shen, and H. Wang, "Capacity of uplink partial overlapping non-orthogonal multiple access for underwater acoustic networks," *IEEE Transactions on Vehicular Technology*, vol. 69, no. 12, pp. 14290–14303, 2020.

[14] H. Esmaiel, Z. Qasem, H. Sun, J. Qi, J. Wang, and Y. Gu, "Wireless information and power transfer for underwater acoustic time-reversed NOMA," *IET Communication*, vol. 14, no. 19, pp. 3394–3403, 2020.

[15] V. Goutham and V. P. Harigovindan, "Full-duplex cooperative relaying with NOMA for the performance enhancement of underwater acoustic sensor networks," *Engineering Science and Technology, an International Journal*, vol. 24, no. 6, pp. 1396–1407, 2021.

[16] J. Cheon and H. S. Cho, "Power allocation scheme for non-orthogonal multiple access in underwater acoustic communications," *Sensors*, vol. 17, no. 11, p. 2465, 2017.

[17] Y. Liu, M. Zhao, L. Xiao, and S. Zhou, "Pilot domain NOMA for grant-free massive random access in massive MIMO marine communication system," *China Communications*, vol. 17, no. 6, pp. 131–144, 2020.

[18] M. Shahab, M. Irfan, M. Kader, and S. Young Shin, "User pairing schemes for capacity maximization in non-orthogonal multiple access systems," *Wireless Communications & Mobile Computing*, vol. 16, no. 17, pp. 2884–2894, 2016.

[19] X. Chen, F. Gong, G. Li, H. Zhang, and P. Song, "User pairing and pair scheduling in massive MIMO-NOMA systems," *IEEE Communications Letters*, vol. 22, no. 4, pp. 788–791, 2018.

[20] S. Mounchili and S. Hamouda, "New user grouping scheme for better user pairing in NOMA systems," in *2020 International Wireless Communications and Mobile Computing (IWCMC)*, pp. 820–825, Limassol, Cyprus, July 2020.

[21] F. Salehi, N. Neda, M. Majidi, and H. Ahmadi, "Cooperative NOMA-based user pairing for URLLC: a max–min fFairness approach," *IEEE Systems Journal*, vol. 15, no. 4, pp. 1–11, 2021.

[22] J. Wang, Y. Li, C. Ji, Q. Sun, S. Jin, and T. Q. S. Quek, "Location-based MIMO-NOMA: multiple access regions and low-complexity user pairing," *IEEE Transactions on Communications*, vol. 68, no. 4, pp. 2293–2307, 2020.

[23] I. Azam, M. B. Shahab, and S. Y. Shin, "User pairing and power allocation for capacity maximization in uplink NOMA," in *2019 42nd International Conference on Telecommunications and Signal Processing (TSP)*, pp. 690–694, Budapest, Hungary, July 2019.

[24] M. Nguyen and L. Le, "NOMA user pairing and UAV placement in UAV-based wireless networks," in *ICC 2019 - 2019 IEEE International Conference on Communications (ICC)*, pp. 1–6, Shanghai, China, May 2019.

[25] M. Pischella and D. Ruyet, "NOMA-relevant clustering and resource allocation for proportional fair uplink communications," *IEEE Wireless Communications Letters*, vol. 8, no. 3, pp. 873–876, 2019.

[26] H. Zuo and X. Tao, "Power allocation optimization for uplink non-orthogonal multiple access systems," in *2017 9th International Conference on Wireless Communications and Signal Processing (WCSP)*, pp. 1–5, Nanjing, China, October 2017.

[27] Y. Li, L. Cai, and K. Su, "Study on power allocation algorithm based on non-orthogonal multiple access in MIMO systems," *Chinese Journal of Computers*, vol. 44, no. 5, pp. 1013–1023, 2021.

[28] S. Hao, Y. Li, S. Zhao, W. Wang, and X. Wang, "Multi-carrier NOMA power allocation strategy based on improved particle swarm optimization algorithm," *Acta Electronica Sinica*, vol. 48, no. 10, pp. 2009–2016, 2020.

[29] M. Zeng, A. Yadav, O. Dobre, and H. V. Poor, "Energy-efficient joint user-RB association and power allocation for uplink hybrid NOMA-OMA," *IEEE Internet of Things Journal*, vol. 6, no. 3, pp. 5119–5131, 2019.

[30] Z. Jing, Q. Yang, M. Qin, M. Mei, and K. Sup Kwak, "Proactive online power allocation for uplink NOMA-IoT networks with delayed gradient feedback," *IEEE Wireless Communications Letters*, vol. 10, no. 4, pp. 869–872, 2021.

[31] J. Zeng, C. Xiao, Z. Li, W. Ni, and R. P. Liu, "Dynamic power allocation for uplink NOMA with statistical delay QoS guarantee," *IEEE Transactions on Wireless Communications*, vol. 20, no. 12, pp. 8191–8203, 2021.

[32] M. Miron-Morin, D. Barclay, and J. Bousquet, "The oceanographic sensitivity of the acoustic channel in shallow water," *IEEE Journal of Oceanic Engineering*, vol. 46, no. 2, pp. 675–686, 2021.

[33] W. Jianping, L. Yingying, W. Chen, G. Guohong, Q. Peixin, and Z. Yu, "SM-UAN: a software-defined underwater acoustic network of multi-controllers for inland waterway systems," *IEEE Access*, vol. 8, pp. 211135–211151, 2020.

[34] J. Wang, G. Gao, P. Qu et al., "A software-defined clustering mechanism for underwater acoustic sensor networks," *IEEE Access*, vol. 7, pp. 121742–121754, 2019.

[35] J. Wang, S. Zhang, W. Chen, D. Kong, X. Zuo, and Z. Yu, "Design and implementation of SDN-based underwater acoustic sensor networks with multi-controllers," *IEEE Access*, vol. 6, pp. 25698–25714, 2018.

[36] J. Wang, L. Ma, and W. Chen, "Design of underwater acoustic sensor communication systems based on software-defined networks in big data," *International Journal of Distributed Sensor Networks*, vol. 13, no. 7, 2017.